A Measurement of the Anisotropy in the Cosmic Microwave Background Radiation at Degree Angular Scales

E. J. Wollack[1], N. C. Jarosik[1], C. B. Netterfield[1], L. A. Page[1], David Wilkinson[1]

Abstract

We detect anisotropy in celestial radiation at degree angular scales between 26 and 36 GHz. The fluctuations have the spectral index of the cosmic microwave background radiation. The root-mean-squared amplitude, Δ_{rms}, of the fluctuations in the data set is $33^{+10}_{-9}\,\mu$K and the average spectral index, β, is $-0.3^{+0.7}_{-1.2}$; for the cosmic microwave background, $\beta = 0$. The 95% confidence upper limit on anisotropy of the polarization is $25\,\mu$K. The most likely amplitude of a Gaussian correlation function, a scan and beam independent measure of the fluctuations, is $41^{+16}_{-13}\,\mu$K with $\beta = -0.3^{+0.7}_{-1.2}$ at a coherence angle of $1\overset{\circ}{.}2$. At these frequencies, some fraction of Δ_{rms} is probably due to anisotropy in free-free emission ($\beta = -2.1$), but our bounds on the spectral index argue that the free-free contribution is not large. Known compact sources and synchrotron radiation do not contribute substantially to the detected anisotropy.

Subject headings: cosmology: cosmic microwave background — cosmology: observations

The author's full names are Edward J. Wollack, Norman C. Jarosik, C. Barth Netterfield, Lyman A. Page, and David T. Wilkinson. Correspondence should be addressed to Lyman Page.

[1]Princeton University, Department of Physics, Jadwin Hall P.O. Box 708, Princeton, NJ 08544

1 Introduction

The discovery of anisotropy in the cosmic microwave background radiation (CMBR) by *COBE* at angular scales 7° and larger (Smoot *et al.* 1992; Bennett *et al.* 1992) and the recent confirmation (Ganga *et al.* 1993) suggest that fluctuations should be measurable at smaller angular scales. On scales less than 7°, measurements have the ability to discriminate between a host of both Gaussian and non-Gaussian models (Coulson *et al.* 1993; Efstathiou *et al.* 1992). We have built an experiment to search for anisotropy at degree angular scales. The beam size, detector technology, and frequency coverage are similar to those used in Gaier *et al.* (1992) and Schuster *et al.* (1993).

2 Instrument and Observing Strategy

The instrument is a total power radiometer that observes in three frequency bands in each of two orthogonal linear polarizations, 'A' (**E** perpendicular to the horizon) and 'B'. Radiation in each polarization is separately amplified with HEMT (High Electron Mobility Transistor) amplifiers (Pospieszalski *et al.* 1988; Pospieszalski 1992) cooled to 12K with a mechanical refrigerator. Commercial circulators and filters define the passbands. The characteristics of the six channels are summarized in Table 1.

All six channels view the sky in a single, approximately frequency-independent, beam with a FWHM $\cong 1^\circ\!.44$ formed by a cold corrugated horn feeding an ambient temperature off-axis parabola. The beam then reflects off a $90\,\mathrm{cm} \times 150\,\mathrm{cm}$ aluminum flat (chopper) oscillating at 3.906 Hz around a vertical axis. The antenna gain at the edge of the chopper is less than -60 dB. The elevation of the beam is fixed at $52^\circ\!.14$, the latitude of the observing site in Saskatoon, SK, Canada. Pointing is accomplished by rotating the entire telescope in azimuth. A large ground screen shields the radiometer from terrestrial emission and reflects unwanted radiation to the welkin. Using both laboratory measurements and astrophysical data, we find a cross-correlation in the noise between channels of the same polarization. The correlation coefficient is 0.3 for A and 0.5 for B. The radiometer is calibrated to 8% absolute accuracy and 2% relative accuracy using cryogenic cold loads, the moon (Keihm 1993), eccosorb, and Cassiopeia A (Baars *et al.* 1977). The calibration uncertainty is not included in the quoted errors.

To measure the sky, the beam is swept in azimuth in a sinusoidal pattern with frequency $f_c = 3.906$ Hz and amplitude $\mathbf{x}_a = 2.^{\circ}45$ on the sky. The center of the pattern, $\mathbf{x}_0(t)$, is positioned $4.^{\circ}9$ west of the north celestial pole (NCP) for 16.4 s, on the NCP for 8.2 s, and $4.^{\circ}9$ to the east of the NCP for 16.4 s. The beam position is thus given by $\mathbf{x}(t) = \mathbf{x}_0(t) + \mathbf{x}_a \cos(2\pi f_c t)$, where $\mathbf{x}_a$ is parallel to the horizon. The absolute pointing error is $0.^{\circ}15$ as determined by frequent measurements of Cassiopeia A. Data taken with $\mathbf{x}_0(t)$ in the East and West are treated independently (not differenced) and the North data are not used. Consequently, the sinusoidal modulation pattern is centered on $\delta = 85.^{\circ}1$. The signal is demodulated in software at the second harmonic of the chop frequency $2f_c$, by multiplying the sampled data stream by a vector of the form, $d(t_i) = -\cos(4\pi f_c t_i)/N$ where t_i is the sample time. The resulting sky pattern resembles a "3-beam-chop" in both East and West positions. [1] After including the effects of beam smearing, the window function (Górski 1993) is well characterized by $\theta_t = 2.^{\circ}45$ and $\sigma = 0.^{\circ}65$. The normalization, N, is chosen so that a 1 K change in a blackbody filling only the positive lobe of the sky pattern gives a detected signal of 1 K.

[1] The chopped beam pattern is approximately $P(\hat{\mathbf{y}}) = (1/N')\sum_{i=1}^{16} d(t_i)exp(-(\cos^{-1}(\hat{\mathbf{y}}\cdot\hat{\mathbf{x}}(t_i))^2)/(2(0.^{\circ}61)^2)$ where $t_i = (i-.5)/(16\,f_c)$ and the normalization, N' is described in the text.

3 Data

The sky was observed for 19 days, between February 21 to March 15, 1993, with the observing plan outlined above. Although the mean value, or 'offset,' of the demodulated signal depends on the channel, as shown in Table 1, it is very stable. No significant correlations between the offset and the receiver temperature or chopper temperature were found and there were no statistically significant drifts. The offsets in Table 1 are subtracted from the data before the analysis; *no drifts were removed.*

Data contaminated by bad weather are cut if the average magnitude of the first harmonic of the sky signal (sensitive to the gradient in atmospheric emission) is greater than η mK. If $\eta < 1.5$ the radiometer is detector noise limited. Note that the signal at f_c (which is dominated atmosphere) is orthogonal to the astrophysical data at $2\,f_c$. With $\eta = 3$, atmospheric fluctuations (at $2\,f_c$) increase the radiometer noise by 40% in A1 and B1, and 20% in A3 and B3 (see Table 1), suggesting that the water line at 22 GHz is the cause of the fluctuations. We also require that there be at least one continuous hour of 'good' data. The data for cut levels of $\eta = 2$, 3, and 5, corrected to thermodynamic temperature, are shown in Figure 1; the analysis uses $\eta = 3$. Of the 450 hours of data, 180 were lost due to bad weather (for $\eta = 3$), 25 were used for instrument maintenance and calibrations, 68 were spent viewing the NCP, and 30 were spent moving the telescope. At 4:30 PM each day, the sun rose above the top of the ground screen and illuminated the chopper, increasing its temperature. Data taken from 3 to 6 PM were discarded causing an addition loss of 33 hours and $\sqrt{2}$ larger error bars in bins 8, 9, 10 and 20, 21, 22. The results do not change if these data are left in. A net of 114 hours of data were used for the analysis.

The East-West wobble is designed to isolate sky signals (which appear with a 12 hour period) from ground, atmospheric, and instrumental effects which have a 24 hour period (Timbie & Wilkinson 1990). Figure 1 shows the data sorted into bins of right ascension. Before combining East and West, the West data are shifted by 12 hours, denoted by E+W_{12}, so that celestial signals add. The binned data show obvious spatial structure that is correlated between channels with different frequency and polarization. The χ^2/ν for A1+B1, A2+B2, and A3+B3 are 91/23, 74/23, 72/23. A correlation analysis shows that the best time lag between the East and West data is 12 hours, not 0 hours as expected for atmospheric or other environmental effects. The combinations of data, E−W_{12}, Day−Night, and A−B should be consistent with zero. After accounting for correlations, the χ^2/ν are 61/51, 61/51, 60/60 for these combinations. Because the data taken during the day are consistent with the data taken at night (Figure 1(d)), we do not believe solar emission or solar heating are contaminating the results. And, because data taken in the East are consistent with data taken in the West (Figure 1(d)), we do not believe differential ground pick-up is contaminating the results. Hence, there is no evidence for contamination of the data by the sun, earth, local interference, or atmosphere.

4 Galactic signals

Near 30 GHz, there are three known celestial sources that compete with the CMBR anisotropy over much of the sky. Fortunately, these have spectral indices ($T \propto f^{\beta}$) different from that of the CMBR's $\beta = 0$. Compact galactic nuclei can have a 'flat' spectral index ($\beta = -2$) (Herbig & Readhead 1992). However, it takes a 1 Jy source in our central lobe to give a signal of 44 μK. To estimate the influence of sources, we use the Kühr *et al.* (1981) survey, complete to 0.25 Jy at 5 GHz, to find 128 sources in the 190 square degrees covered by this experiment. Using measured indices wherever possible and 'flat' spectra otherwise, the signal expected from these sources was estimated and plotted in Figure 1(e). The *rms* amplitude of the source contribution is less than 8 μK, too small to account for the signal we see. Estimated signals from the six strongest sources are shown in boxes. No corrections are made for the sources.

Diffuse Galactic synchrotron emission has a nominal spectral index of $\beta = -2.8$. Using this value to extrapolate radio maps at 408 MHz (Haslam *et al.* 1982) and 1.4 GHz (Reich & Reich 1986) to 30 GHz, and convolving the maps with our beam, gives the curves in Figure 1(e). The *rms* amplitude of the estimated synchrotron signal is less than $5\,\mu$K. However, a spatial variation in the spectral index of the order $\delta\beta(x) \approx 0.05$ matched to our observing pattern could cause $30\,\mu$K fluctuations in the synchrotron component at 30 GHz. Our best argument against this source is our measurement of $\beta = -0.3^{+0.7}_{-1.2}$.

Diffuse free-free emission ($\beta = -2.1$) is expected to be a serious problem at 30 GHz (Wilkinson 1982; Bennett *et al.* 1992). At 408 MHz and 1.4 GHz, synchrotron emission masks free-free emission, so indirect methods must be used to estimate the emission measure. For example, Reynolds (1992) has mapped $H\alpha$ in a $10^\circ \times 12^\circ$ region. Taking that map, made at $b = -22^\circ$, as representative of our patch and assuming that $\delta H\alpha/H\alpha = 0.5$ in a patch *matched* to our search pattern (which is very pessimistic) one predicts $\Delta_{rms} \approx 35\,\mu$K, the size of the signal. To explain a $\Delta_{rms} \approx 30\,\mu$K at 30 GHz, one must extrapolate *all* the fluctuations in the 1.4 GHz map with $\beta = -2.1$. Spectral index fluctuations of $\delta\beta(x) \approx 0.01$ (matched to our observing pattern) would contribute a $\Delta_{rms} \approx 10\,\mu$K if 20% of the flux of the 1.4 GHz map is free-free emission. Because so little is known about Galactic free-free emission at 30 GHz, β *must be measured* to discriminate between CMBR anisotropy and spatial variations in free-free emission.

5 Likelihood analysis for anisotropy

The Bayesian method with a constant prior (Readhead *et al.* 1989, Bond *et al.* 1991) is used to test for fluctuations in the CMBR, though the treatment is extended here to find both the root-mean-squared amplitude, Δ_{rms}, of the fluctuations in the data and the spectral index, β of the fluctuations. We use much of the implementation and notation in Cheng *et* *al.* (1993). The sky signal in a bin is $s_i = \int H_i(\mathbf{x})T(\mathbf{x})d\mathbf{x}$, where T is the temperature of the sky model and H_i is the oriented beam profile for the whole 1 hour bin. The full covariance matrix is:

$$\begin{aligned} M_{ij}^{kl} &= < s_i^k\, s_j^l > + D_{ij}^{kl}\sigma_i^k\sigma_j^l \\ &= \int d\mathbf{x}_1\, d\mathbf{x}_2\, H_i^{ew}(\mathbf{x}_1) H_j^{ew}(\mathbf{x}_2) C(|\mathbf{x}_1 - \mathbf{x}_2|, \beta) + D_{ij}^{k\,l}\sigma_i^k\sigma_j^l. \end{aligned} \quad (1)$$

This 288×288 matrix is built of 36 similar 48×48 sub-matrices. Each sub-matrix separately accounts for data taken in the East and West. The indices i and j range from 1 to 48 and denote the sky bin; the k or l superscript denotes a channel with a given frequency and polarization. The ew superscript reminds one to choose the correct H for a given bin because the East and West profiles are slightly different with respect to the celestial sphere. Variations in sky temperature are modeled as arising from a single fluctuating component with a spectrum $\propto f^{\beta}$. The correlation function is $C(|\mathbf{x}_1 - \mathbf{x}_2|, \beta) = (f^k f^l)^{\beta}\, C_0^2\, c(\theta)$, where f^k is the frequency of channel k normalized to 27.5 GHz and C_0 is the amplitude of the correlation function. The data covariance matrix $D_{ij}^{k\,l}$ is diagonal in each of the 36 sub-matrices; it accounts for the HEMT induced channel-to-channel correlations, atmospheric correlations, and the statistical weight of each datum. The only instrumental effect not accounted for in $\mathbf{M}$ is the offset subtraction from each channel, this leads to an increase in the error bar of $\approx 1/21$; the quoted errors have been adjusted accordingly. Finally, the likelihood of the data set is proportional to $\exp(-\mathbf{t}^{\mathbf{T}}\, \mathbf{M}^{-1}\, \mathbf{t}/2)/|\mathbf{M}|^{1/2}$ where $\mathbf{t}$ is the vector containing the data.

Two separate measures of the fluctuations are presented. The most likely Δ_{rms} and index of the data are found by normalizing $< s_i^k\, s_j^l >$ to 1 on the diagonal with $C_0 = 1$, $c(\theta) = \delta(\theta)$, and $\beta = 0$ and then varying C_0, which in this case is Δ_{rms}, and β to maximize the likelihood. The results are plotted in Figure 2; the most likely values are $\Delta_{rms} = 33^{+10}_{-9}\mu$K and $\beta = -0.3^{+0.7}_{-1.2}$. The error bars bracket the 16% to 84% integral over the likelihood, analogous to 1σ. The 90% confidence interval on β is -2.2 to $+1.0$. A limit on the polarization anisotropy is obtained by analyzing data from the difference in polarizations, A$-$B; the 95% confidence upper limit on such fluctuations with $\beta = 0$ is $25\,\mu$K. In the second method, a Gaussian correlation function, $C(|\mathbf{x}_1 - \mathbf{x}_2|, \beta) = (f^k f^l)^\beta C_0^2 \exp(-\theta^2/2\theta_c^2)$, with $\theta_c = 1\overset{\circ}{.}2$ is used in equation (1). The result is $C_0 = 41^{+16}_{-13}\,\mu$K and $\beta = -0.3^{+0.7}_{-1.2}$. This value is independent of the observing strategy and may be compared directly to the results from other experiments.

6 Discussion

The most likely value for the spectral index is very close to that expected for the CMBR, though free-free emission is excluded with only 90% confidence. The relatively higher probability for more negative indices in Figure 2 hints at the presence of low levels of free-free contamination in our field. Still, the most parsimonious description of the data is that fluctuations in the CMBR dominate our sky signal.

To relate the sky signal to theory, a model power spectrum is integrated over the window function. From Górski (1993), predictions based on *COBE* give $\Delta_{rms} \approx 30\,\mu$K, in agreement with our measurement. Additionally, Bond (1993) finds $\Delta_{rms} \approx 40\,\mu$K. In a similar experiment done at the South Pole, Gaier *et al.* (1992) give $C_0 = 38\ \mu$K as the 95% upper limit on the amplitude of the Gaussian correlation function with a coherence angle of $1\overset{\circ}{.}2$. Schuster *et al.* (1993) have a detection at $23^{+22}_{-10}\,\mu$K (2σ error bars), but obtain $\beta = -2^{+1.5}_{-1.8}$. Both of these results are roughly consistent with our $41^{+16}_{-13}\,\mu$K. In comparing the South Pole and Saskatoon experiments we note that: 1) the South Pole work is done at a Galactic latitude of $-63°$, where one expects less Galactic free-free emission; 2) we cover over four times as much sky as Schuster *et al.* (1993); 3) in our data, the sky signals appear well correlated between frequencies and fluctuations are present throughout the data set; the eye cannot distinguish between these data and CMBR simulations made with normally distributed random numbers; 4) the South Pole atmosphere is colder and more quiet but 3-beam chopping provides better atmospheric rejection and a much more stable baseline than the 2-beam chop used in the South Pole experiments. The experiments have similar overall sensitivity but different susceptibility to systematic effects.

7 Acknowledgments

We thank John Kulvicki, Young Lee, and the Princeton shop for helping us build the 'BigPlate' experiment. George Sofko and Mike McKibben at the University of Saskatchewan's Institute for Space and Atmospheric Studies and Larry Snodgrass at the Canadian SRC provided valuable assistance with our Saskatoon operations. The remarkable HEMT amplifiers were provided by Marian Pospieszalski and Mike Balister at NRAO; these devices are revolutionizing sensitive cm-wave radiometry. Conversations with Ruth Daly were helpful for understanding sources, and Henry Wolkowicz taught us efficient numerical methods. We also thank Dick Bond, Todd Gaier, Josh Gundersen, and Phil Lubin for useful discussions. This work was supported by NSF grant PH89-21378 and NASA grants NAGW-2801 and NAGW-1482.

The data, window function, correlation coefficients, and beam profile are publicly available. They may be obtained from PUPGG.PRINCETON.EDU using 'anonymous FTP;' the directory is [.JAROSIK]. The data, along with a more complete description of the analysis, will be presented in an upcoming paper.

Table 1: Radiometer Passbands, Sensitivity, and Offsets

Chan.	ν^a [GHz]	$S_{\rm lab}{}^b$ [mK sec$^{\frac{1}{2}}$]	$S_{\rm sky}{}^c$ [mK sec$^{\frac{1}{2}}$]	$E_{\rm offset}{}^d$ [μ K]	$W_{\rm offset}$ [μ K]	$\Delta_{rms}{}^e$ [μ K]	$\bar{\sigma}^f$ [μ K]
A1	$26-29$	1.1	1.6	-36 ± 7	-17 ± 7	49	37
A2	$29-32$	1.5	1.9	-67 ± 10	-53 ± 10	66	47
A3	$32-35$	1.3	1.6	-68 ± 8	-83 ± 8	54	38
B1	$26-29$	1.1	1.5	-279 ± 7	-283 ± 7	45	35
B2	$29-32$	1.3	1.7	-314 ± 8	-320 ± 8	49	37
B3	$32-36$	1.4	1.7	-371 ± 8	-385 ± 8	42	40

[a] 3 dB bandwidths. The full HEMT bandwidth is divided into three sub-bands to obtain spectral information.

[b] Receiver noise (total power) achieved in the lab at 8 Hz using a 15 K cold load. The increase over the ideal 0.9 mK sec$^{\frac{1}{2}}$ is due to imperfect passbands and "$1/f$" noise in the HEMT amplifier. The error is ± 0.1 mK sec$^{\frac{1}{2}}$.

[c] System noise at 8 Hz while observing. These results are for $T_{sky} = 15\,\mathrm{K}$ with a cut level of $\eta = 3$ (see section 3). The sensitivity to CMBR fluctuations is 3 times worse because of the observing pattern. The error is ± 0.1 mK sec$^{\frac{1}{2}}$.

[d] Polarized emission from the chopping plate is the dominant contribution to the offset.

[e] Root-mean-squared amplitude of the combined East and West data when binned by RA ($\eta = 3$).

[f] The average error bar per point for combined East and West when binned by RA ($\eta = 3$).

REFERENCES

Bennett, C. L. *et al.* 1992, ApJ, 396, L7

Baars, J. W. M., Genzel, R., Pauliny-Toth, I. I. K., & Witzel, A. 1977, A&A, 61, 99-106

Bond, J. R., Efstathiou, G., Lubin, P. M., & Meinhold, P. R. 1991, Phys. Rev. Let., 66, 2176

Bond, J. R. 1993, Private Communication. This number is a rough approximation for $\Omega_b = 0.05$, $h = .5$, and a Peebles-Harrison-Zel'dovich power spectrum. It has not yet been subject to a rigorous analysis.

Cheng, E. S., Cottingham, D. A., Fixsen, D. J., Inman, C., Kowitt, M., Meyer, S. S., Page, L. A., Puchalla, J., Silverberg, R. 1993, ApJ, submitted

Coulson, D., Pen, U. & Turok, N. 1993, Nature, submitted

Efstathiou, G., Bond, J.R., & White, S.D.M. 1992, MNRAS, 252, 1

Ganga, K.M., Cheng, E.S., Meyer, S.S., & Page L.A. 1993, ApJ, 410, L57

Gaier, T., Schuster, J., Gundersen, J., Koch,T., Seiffert, M., Meinhold, P. R., & Lubin, P. M., 1992, ApJ, 398, L1

Górski K. 1993, ApJ, 410, L65

Haslam, C. G. T., Salter, C. J., Stoffel, H., Wilson, W. E., 1982, A&AS, 47,1

Herbig, T. & Readhead, A. C. S., 1992, ApJS, 81, 83

Keihm, S. J., 1993. Private communication. We use the model from the Jet Propulsion Laboratory in Pasadena, CA for the Moon's temperature. The model accounts for temperature distribution across the Moon given the phase. After correcting for compression in the detectors, we find the moon is too cold by 10% with respect to Cassiopeia A and laboratory calibration.

Kühr, H., Pauliny-Toth, I.I.K., Witzel, A., Schmidt, J., 1981, AJ, 86, 854-863 (S5 survey, $\delta > 70°$)

Pospieszalski, M. Weinreb, S., Norrod, R., & Harris, R. 1988, IEEE, MTT, 36, 552

Pospieszalski, M. 1992, IEEE, MTT-S, 1369

Readhead, A. C. S., Lawrence, C. R., Myers, S. T., Sargent, W. L. W., Hardebeck, H. E., & Moffet, A. T. 1989, ApJ, 346,566

Reich, P., & Reich, W. 1986, A&AS, 63, 205

Reynolds, R. J. 1992, ApJ, 392, L35

Schuster, J., Gaier, T., Gundersen, J., Meinhold, P., Koch,T., Seiffert, M., Wuensche, C., & Lubin, P. 1993, ApJ, 412, L47

Smoot, G. F. *et al.* 1992, ApJ, 396, L1

Timbie, P. T., & Wilkinson, D. T., 1990, ApJ, 353, 140

Wilkinson, D. T., 1982, Phil. Trans. R. Soc. London. A, 307, 55

This manuscript was prepared with the AAS WGAS LATEX macros v2.2

8 Figure 1 Caption

The data, referenced to the top of the atmosphere, and known foreground emission. (a), (b), and (c) contain the data for A1+B1, A2+B2, A3+B3 with East and West combined. Each panel shows three cut levels, $\eta = 2, 3, 5$; the amounts of data at each level are in the ratios 0.6:1:1.4 respectively. Note the agreement despite choice of η. (d) contains the data for the East (triangle) and West (squares) independently. The unfilled symbols were taken during the day and the filled ones at night. (e) contains the 408 MHz (solid) and 1.4 GHz (long dash) maps convolved with our sky coverage and scaled to our frequency with $\beta = -2.8$. Also shown is the predicted flux from all known sources convolved with our beam. The heights of the five boxes give the error in magnitude of six prominent extra-galactic sources, 3C61.1, 0454+844, 0615+820, NGC6251, 1637+826 (also in 4) and 2342+821. The galactic latitude for 0^h is $22°$, for 8^h is $28°$, for 14^h is $32°$, and for 20^h is $26°$. All error bars include the appropriate correlations.

9 Figure 2 Caption

Contour plot of the likelihood in the $\Delta_{rms} - \beta$ plane. The solid lines are for the $\eta = 3$ data analyzed as described in the text. The values of the contours are 0.1, 0.3, 0.5, 0.7, 0.9. The '1σ' error bars describe the span between 16% and 84% of the total *integrated* likelihood and the maximum of the likelihood is at ($33\,\mu$K, -0.3). The dotted lines are the likelihood contours for A$-$B, the polarization signal; the 0.9 contour is nearest the origin. The 95% confidence upper limit on anisotropy in the polarization with $\beta = 0$ is $25\,\mu$K.

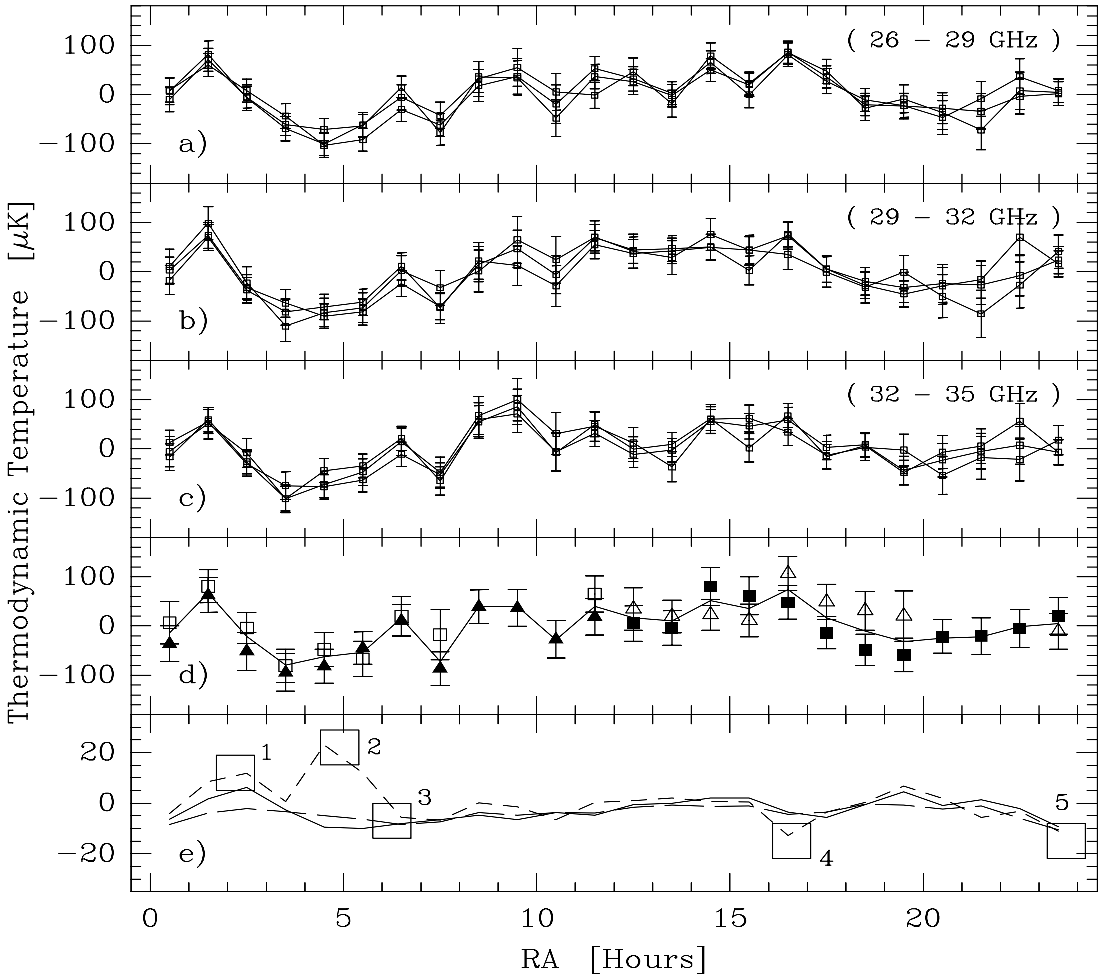

(26 – 29 GHz)
(29 – 32 GHz)
(32 – 35 GHz)
a)
b)
c)
d)
e)
1
2
3
4
5
100
0
−100
20
0
−20
Thermodynamic Temperature [μK]
0
5
10
15
20
RA [Hours]

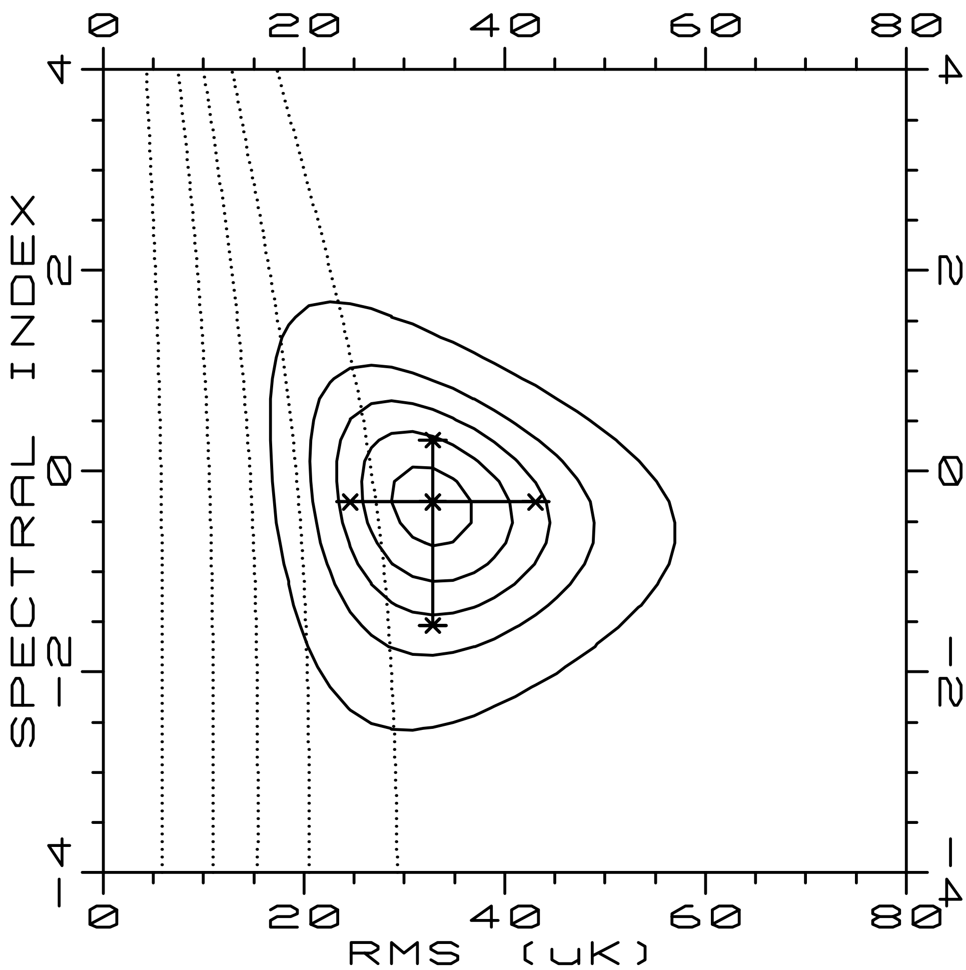
SPECTRAL INDEX
RMS (uK)
0
20
40
60
80
4
2
0
-2
-4